Overview and Analysis of PM Starter/Generator for Aircraft Electrical Power Systems

Zhuoran Zhang, *Senior Member, IEEE*, Jian Huang, Yunyi Jiang, Weiwei Geng and Yanwu Xu
(Invited)

***Abstract*—More Electrical Aircraft (MEA) which replaces the hydraulic and pneumatic power by electrical power leads to reducing emissions and fuel consumption. The MEA concept has led to a growing use of the starter/generator (S/G) system. Permanent magnet (PM) machines have been gaining interests for aircraft S/G system application over the last few years. This is mainly due to the several advantages, including high power density, high efficiency and high speed ability. The shortcoming of the PM machines is the de-excitation problem in case of a failure, which is a main issue for the aircraft application. However, by using a PM machine with high reactance or multiphase configuration, the fault-tolerant ability can be improved. In terms of the aircraft S/G system, this paper is going to present a comprehensive analysis of PM machines. Firstly, the state-of-the-art of PM starter/generator (PMS/G) is summarized and the basic structure of PMS/G system is analyzed. Next, key technologies of the PMS/G system are summarized and analyzed. Finally, a flux weakening fault protection strategy that is used to suppress the turn-to-turn short circuit (SC) current is studied, simulated and verified. With the breakthrough of key technologies based on the development of high temperature electromagnetic material and high temperature power electronics, the PMS/G will be a potential candidate for aircraft S/G system including the embedded power generation system.**

***Index Terms*—Fault tolerant, flux weakening strategy, high reactance machine, more electrical aircraft, multiphase, permanent magnet machine, starter/generator.**

I. INTRODUCTION

THE framework of the aircraft electrical power system (EPS) can be classified into five systems, namely low voltage DC system (LVDC), high voltage DC (HVDC) system, constant speed constant frequency (CSCF) system, variable speed constant frequency (VSCF) system and variable speed variable frequency (VSVF) system. Among these, HVDC system has high reliability, high efficiency, light power distribution, and is easy to run in parallel and realize uninterrupted power supply transition [1]. As the consequence of gradually substituting the hydraulic, pneumatic and mechanical system with electrical power system, there is an obvious trend towards the increasing demand of electrical power. Increasing the voltage rating is helpful to reduce the current and joule loss. In other words, it means that the feeding cable will reduce the wire diameter, thus decreasing the weight and volume of the onboard power supply system [2].

The development of the EPS paves the way for S/G technology. The S/G combines the starting function and generating function into one machine which can save weight and space. It is one of the key technologies to implement the more/all electric aircraft (M/AEA). The S/G needs to satisfy two basic requirements, namely to accelerate the engine and to generate electrical power. When functioning as a starter, the S/G accelerates the engine to the self-sustaining speed. Afterwards, the S/G in turn driven by aircraft engine can supply power to the onboard loads in generating mode.

Three-stage brushless synchronous starter/generator has been proved to be a mature candidate as the S/G for the high power factor in a wide speed range and reliable de-excitation ability in case of a failure[3]. However, due to the rotating rectifiers and windings on the rotor, the structure of the rotor is too complex to operate at higher speed, which decreases the reliability. In addition, the starting control strategy is also a difficult point.

PMS/G has been considered in automobile application for its high power density, high efficiency and high speed ability, especially the interior permanent magnet (IPM) machine [4]. Compared to automotive application, PMS/G is restricted in aircraft application mainly due to the de-excitation problem under fault condition and the risk of the irreversible demagnetization in high temperature. Thus, a lot of work has been done on the machine side as well as power converter side to meet the critical requirements and broaden the application.

With the development and application of the rare earth permanent magnet materials and high temperature power electronic devices, the power capacity of the aircraft PM generator is getting larger gradually. So far, the PM machines are not only adoptable in the flight control and engine control system with low power ratings, but are also gaining more interests for the primary electrical power system of aircraft.

This paper presents an overview of the PMS/G and summarizes of the relevant key technologies for aircraft application. The basic structure of the PMS/G system is also proposed. In order to suppress the turn-to-turn SC current, a flux weakening fault protection strategy is presented.

This work was supported in part by National Natural Science Foundation for Excellent Young Scholar of China under Award 51622704, Jiangsu Provincial Science Funds for Distinguished Young Scientists under Award BK20150033.

The authors are with the Center for More-Electric-Aircraft Power Systems, Nanjing University of Aeronautics and Astronautics, Nanjing, china.(e-mail:apsc-zzr@nuaa.edu.cn;jianhuang_nuaa@163.com; jiangyunyi_nuaa@163.com; gww0424@163.com;xuyanwu1990@163.com).

II. State-of-the-art and Development of PM Starter/Generator for Aircraft EPS

A typical PMS/G system is composed of PMS/G, bi-directional converter and corresponding controller. In [5], the overall structure of PMS/G system is investigated. The transition of the operation mode between starting and generating is realized according to the machine speed. Different flux weakening methods are discussed. Due to the simple structure and independence on the load condition, a direct flux weakening strategy is adopted to adjust the AC terminal voltage in generating mode and to implement the acceleration in starting mode. The command torque current is calculated based on the principle of power balance and the dc-link current demand is calculated according to the droop characteristic for the sake of paralleling with other power sources connected to the dc bus. However, the approach is mainly suitable for surface mounted PM machines (SPMM) since the electromagnetic torque is determined only by the torque current component of SPMM.

In [6], a different control structure of PMS/G system is presented. The command torque current is the output of a PI controller of the dc current loop. This approach is applicable to different rotor structures, not limited to SPMM. In [7], another flux weakening method based on the control structure discussed in [6] is proposed .The method is named as advanced angle control, which means the reference current vector is shifted by an angle to get the demagnetizing current. The disadvantage is that there is no current vector under no load.

Some typical PMS/Gs are designed and studied in literature. In [8], a PMS/G is designed with power of 45kW at 32krpm for the 270VDC electrical power system. To minimize the core losses and converter losses, the slot pole combination is chosen as 36/6 and a distributed winding configuration is adopted that can reduce the harmonic component of electromotive force (EMF). The permanent magnets are arranged in Halbach structure with samarium cobalt magnet (Sm_2Co_{17}) material. The structure is optimized to prevent demagnetization risk when operating in worst-case rotor temperature. The carbon fiber sleeve which is characterized with lower eddy current losses compared to inconel sleeve is adopted in order to retain the permanent magnets at high speed. A direct oil cooling method called wet stator is identified to maximize the machine efficiency as well as power density. The oil is also used for the lubrication of the gearbox. A stator can is introduced into the air gap to isolate the stator region from the rotor, which could make the rotor spins in a dry condition to keep windage losses manageable. The cross section of the machine and the prototype of stator and rotor are shown in Fig.1.

Different rotor structures such as Inset PM, consequent pole (CP) PM, interior PM (IPM), spoke type PM are compared in [9]. Both the stator and the rotor diameter are kept constant, as well as the core material, electrical, magnetic, thermal and structural limitations. Finally, spoke type machine has been chosen for prototyping, considering the comparatively high efficiency for minimal rotor losses and magnets volume. The cross section of the compared rotor structures are shown in Fig.2.

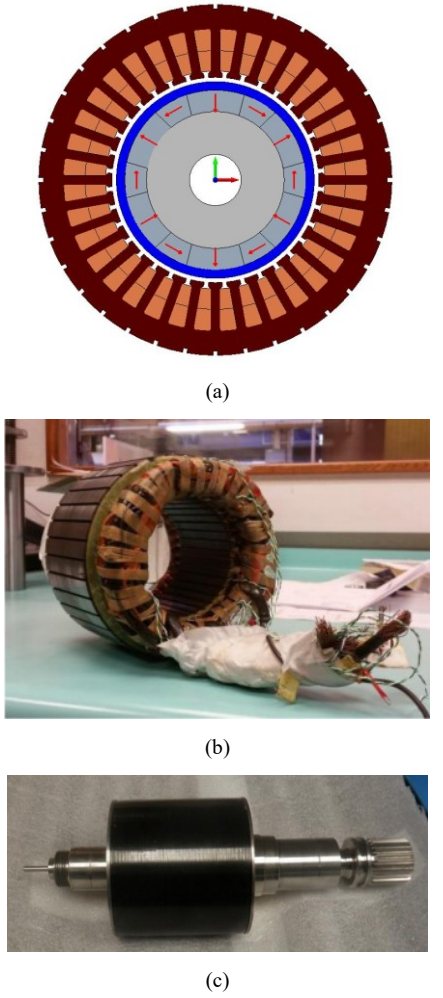

Fig. 1. S/G for HVDC power system(a) Cross section of 36-slot, 6-pole PM machine (b) stator structure (c) rotor with retaining sleeve [8].

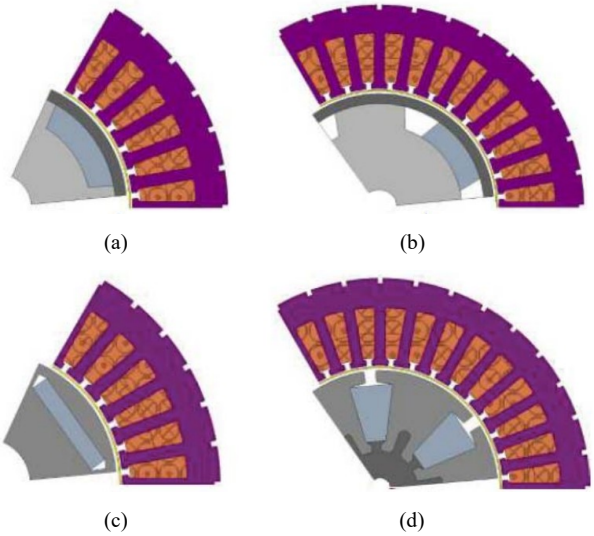

Fig. 2. Cross sectional view of (a) inset PM machine (b) consequent pole PM machine (c) IPM machine and (d) spoke-type PM machine [9].

In [10] [11], a detailed design of PMS/G is presented. The key specifications are given in Table I. To limit the SC current, the reactance of the machine is designed to be high. Meanwhile,

TABLE I
A 6KW PMS/G SPECIFICATIONS

Parameter	Requirement
Generator power	6kW
Generator speed	6000-12000r/min
Generator efficiency	>93%
Starting torque (0-40% speed)	30Nm
Starting duration	15-25s
Starting copper losses	<2kW
Maximum fault losses	<600W
Cooling	Forced air

TABLE II
SPECIFICATIONS OF A SURFACE MOUNTED PMS/G

Parameter	Requirement
Generator power	5kW
Maximum speed	24000 r/min
Generator speed	50-100%
Generator efficiency	>90%
Starting torque	20Nm
Cooling	Shaft mounted fan

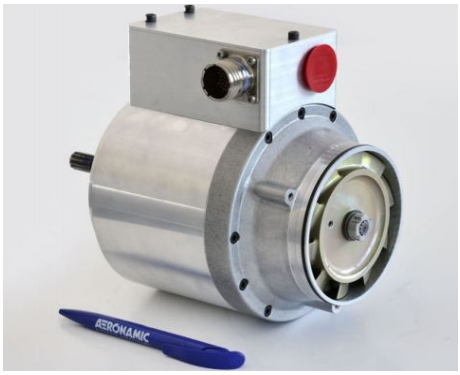

Fig. 3. The prototype of the 5kW PMS/G [12].

the high reactance also affects the starting performance of the machine. Thus, a trade-off needs to be considered in the design stage.

A surface mounted PMS/G is also designed in [12]. Detailed information is given in Table II. The winding AC losses can be reduced by using several thinner strands in parallel. The rotor eddy-current losses can be reduced through two ways, the segmentation of the permanent magnets and adoption of carbon fiber retaining sleeve. A prototype of the design is shown in Fig.3.

In [13], a comparison between three-level converter and two-level converter is presented for PMS/G system. In starting mode, the losses of the two converters are almost the same, but the loss components are quite different. The losses of two-level converter include conduction losses and switching losses of the IGBTs. While the losses of three-level converter are mainly the conduction losses of the IGBTs. In generating mode, current will flow mostly through the diodes and the conduction losses

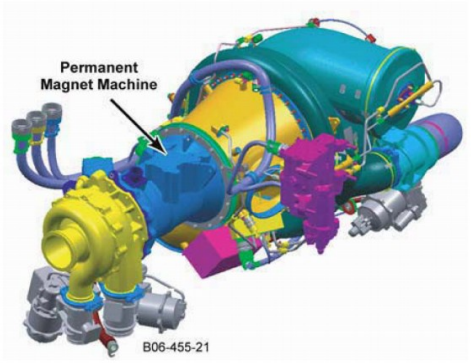

Fig. 4. PTMS for JSF Incorporating a HRPMM [15].

Fig. 5. Turbine Power Unit [16].

are much lower for the two converters. But the switching losses of IGBTs and diodes are much lower with the three-level converter. Thus, three-level converter is adopted for lower losses in generating mode.

In [14], the aircraft power and thermal management system (PTMS) developed by Honeywell is analyzed in detail. The PTMS combines the function of an auxiliary power unit (APU), emergency power unit (EPU), environment control system (ECS), and thermal management system (TMS) in one integrated system which results in a substantial reduction in overall aircraft size and weight. The practical application of PTMS is presented in [15]. Lockheed Martin Joint Strike Fighter (JSF) uses the technology of PTMS and a high reactance PM machine (HRPMM) is selected to be incorporated on the same shaft of the gas turbine engine and a cooling turbine. Conventional oil-lubricated ceramic bearings are employed and the maximum speed reaches 62krpm. The system delivers up to 140kW, 270VDC power. A 3-D model of PTMS is shown in Fig.4.

In [16], A HRPMM is designed under the effort of Lockheed Martin Aeronautics and Honeywell Aerospace-Torrance for the turbine power unit (TPU) which combines the foil bearings, turbine shaft seal, HRPMG and reaction chamber with a turbine wheel and housing. The generator is designed to provide 142 kW over a range of speed from 50400 rpm to 61600rpm. The TPU is shown in Fig.5.

In [17], a topology of high performance power generation systems using HRPMM is presented. The topology shown in

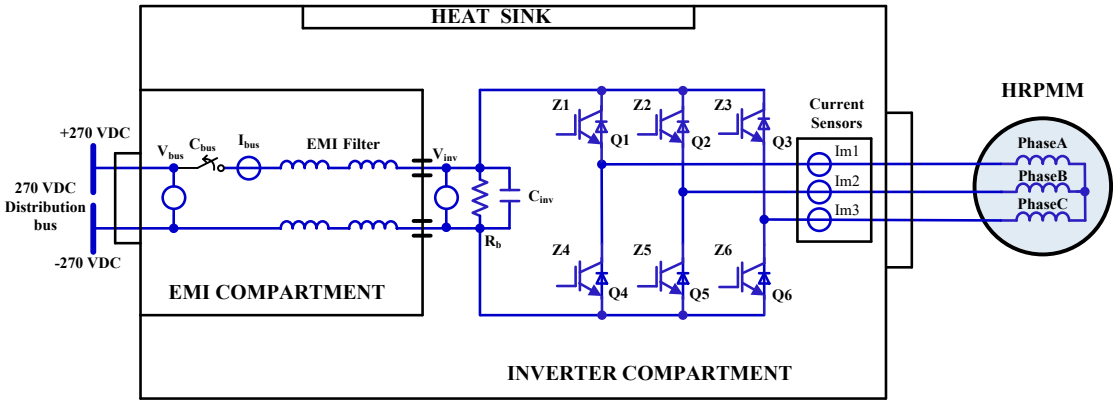

Fig. 6. Basic topology of HRPMM based S/G system [17].

Fig.6 is comprised of three phase bridge converter, DC link capacitor bank, EMI filter, contactor, current and voltage measurement devices. The contactor is not a mandatory component for all applications. It is demonstrated that the reactance of the machine is selected such that the short circuit current of the machine satisfies the requirement of the DC bus short circuit current. A typical ratio between the short circuit current of the DC bus and the phase current.is 1.35. The ratio may vary depending on the components selected for the three phase bridge and the EMI filter.

In [1], another practical application of the PMS/G is presented. The US air force initiated an advanced development program to flight test a 60kVA VSCF S/G system for the A-10 aircraft. This program demonstrated that PM machines could electrically start a turbine engine and produce required power for VSCF power system.

III. Basic Structure and Principle of PM Starter/Generator System

The torque-speed characteristic of aircraft PMS/G is shown in Fig.7. PMS/G functions as a motor during the engine start and supplies electrical power from standstill to cutoff speed ω_{cutoff}. When the machine reaches the minimum generation speed ω_{min}, the system turns into generating mode which supplies power to the electrical loads. So the whole system should satisfy the requirements both at starting mode and generating mode, meanwhile the operation controller can automatically select the working mode according to the machine speed. The control structure of the PMS/G for HVDC power system is shown in Fig.8.

As can be seen from Fig.8, the PMS/G system is comprised of PMS/G, bi-directional converter, DSP controller, IGBT drive circuit, etc. The DSP controller is a key unit that implements main control functions such as starting control, generating control, S/G transition control and flux weakening control. Onboard or ground power supplies power to PMS/G during starting mode and K1 is turned off once the PMS/G reaches the cutoff speed. After stabilization of DC voltage, K2 is on in order to deliver power to the load.

When PMS/G operates at the relatively low speed in starting mode, the vector control strategy with i_d =0 is adopted. A direct

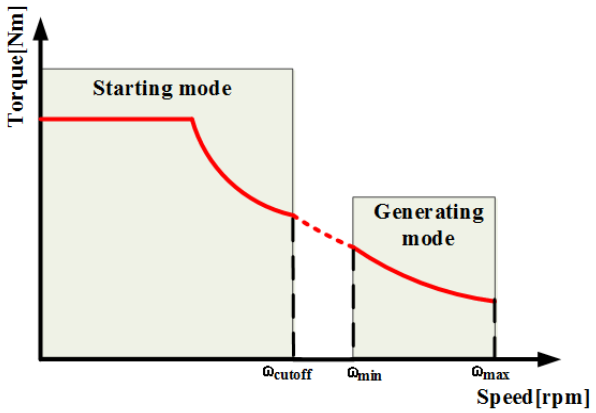

Fig. 7. Torque-speed characteristic of S/G system.

current control method that the command demagnetization current is directly controlled by a PI controller is adopted at high motoring speed. In order to minimize the system losses, the maximum torque per ampere (MTPA) control strategy can also be used.

When PMS/G operates at generating mode, the DC voltage is obtained by the cascaded pulse width modulation (PWM) converter. Detailed analysis is shown in the next section.

IV. Key Technologies of the PMS/G System

The key technologies of PMS/G system are summarized and analyzed as follows. Provided that the key technologies are fully demonstrated and verified, the implementation of the PMS/G system for aircraft applications will be very attractive.

A. Generation control technology

Detailed information of the PMS/G system schematic diagram is illustrated in Fig.9. In the starting mode, machine speed is the controlled quantity, while in the generating mode, DC voltage is the controlled quantity. The S/G transition control signal is used to control the transition process. K is a control method for implementing the transition, which can be considered as a switch with multiple input ports and single output port. When the machine speed reaches the cutoff speed ω_{cutoff}, K_1 is off and the signal K_{2index} is used to control K with

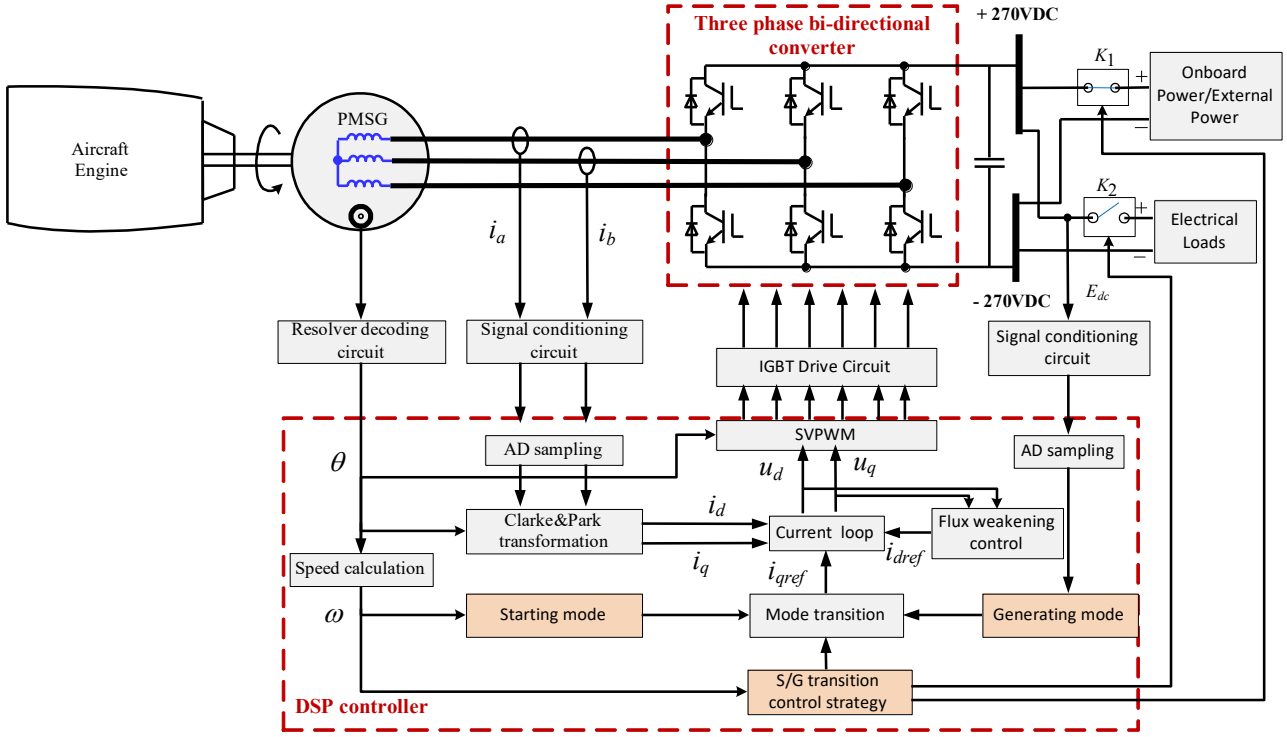

Fig. 8. Block diagram of the PMS/G system.

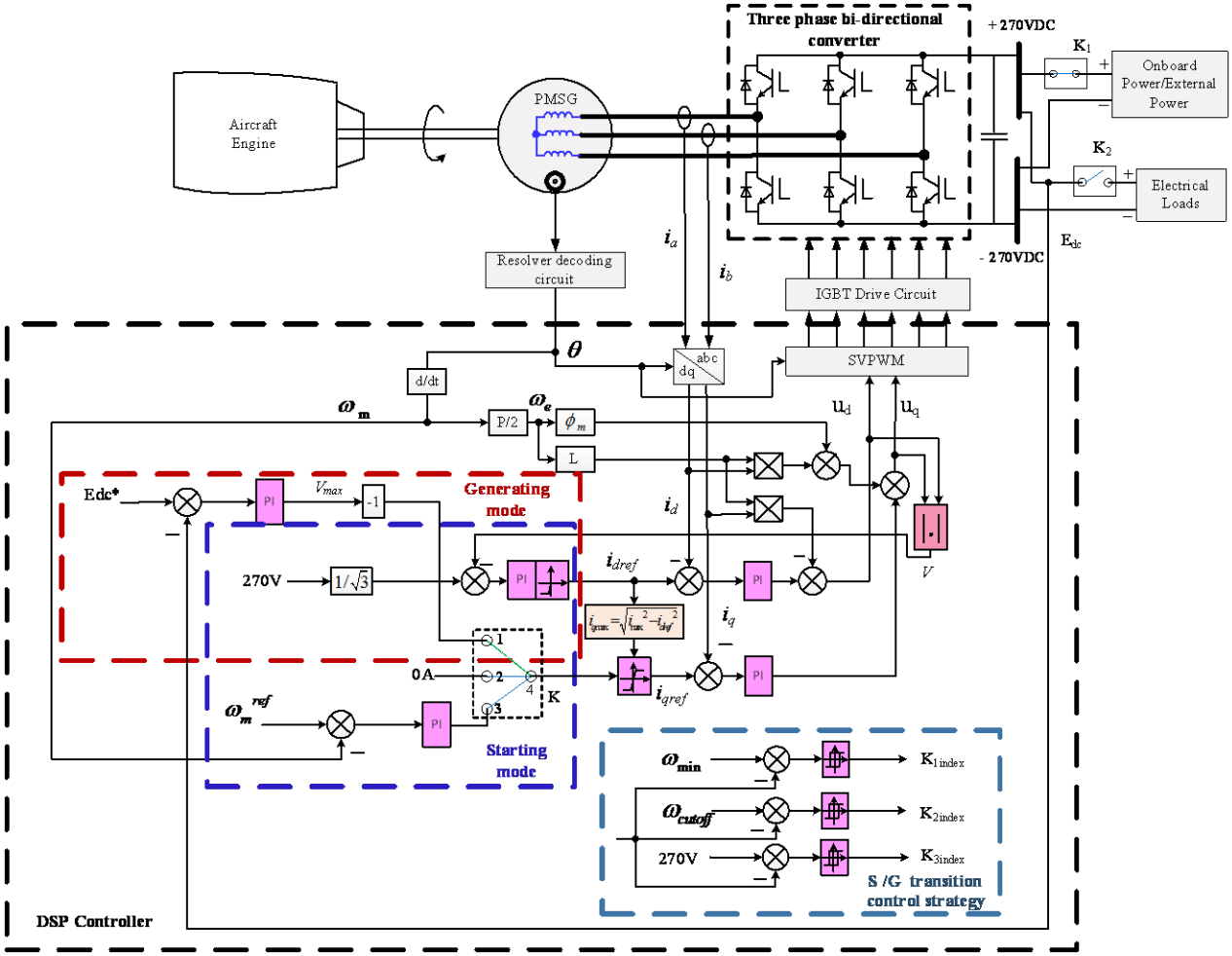

Fig. 9. Schematic diagram of the PMS/G system.

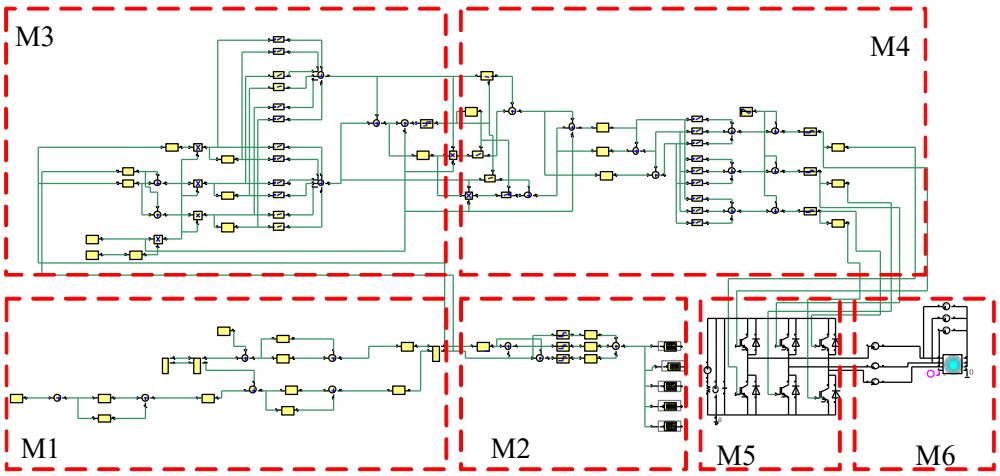

Fig. 10. The PM generation system based on PWM rectifier.

the output port 4 connecting to the input port 2. When the engine speed reaches the speed $c\omega_{min}$, the signal K_{1index} is used to control K with the output port 4 connecting to the input port 1. Parameter c is a coefficient determined by the engine, usually 0.9. When the measured DC voltage is stable and reaches 270VDC, the signal K_{3index} is used to turn K2 on.

To analyze the basic principle of generation control, a model of a PMSM and a three phase PWM rectifier is established shown in Fig.10.Where, M1 contains the voltage and current regulation closed loops, M2 is the calculation of section, M3 is the calculation of conducting time of the IGBTs, M4 is PWM chopping module, M5 is three phase bridge converter, M6 is the PMS/G.

The phase current under rated resistance load at 8000rpm is shown in Fig.11 (a). The phase current is sinusoidal shaped with SVPWM control. Fig.11 (b) shows the output voltage with low voltage ripple of the generation system. Fig.11 (c) depicts the relationship between the speed and the output voltage under light load.

The aircraft S/G always operates at a wide speed range around a ratio of 1:2 in generating mode. The voltage can be regulated to 270VDC when the speed changes from 2000rpm to 12000rpm, which satisfies such requirement. The output voltage is limited by the maximum output power capability when the speed is less than 2000rpm. When the speed exceeds 12000rpm, the terminal voltage is out of control while the converter functions as a pure diode rectification.

B. Flux weakening control technology

Generally, the maximum AC voltage of the machine is limited by the DC bus voltage. Thus, the flux weakening control method is required to adjust the AC terminal voltage of the machine in generating mode. Meanwhile, flux weakening control may be needed to achieve high speed in starting mode, which depends on the drag-speed characteristic of the engine.

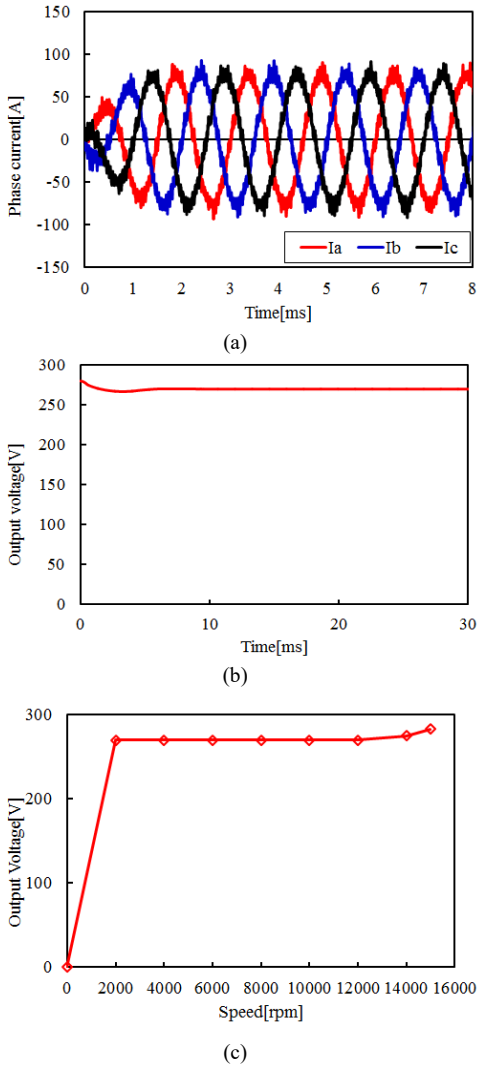

Fig. 11. (a) The phase current under rated load at 8000rpm (b) The output voltage under rated load at 8000rpm (c) Output voltage and speed relationship under light load.

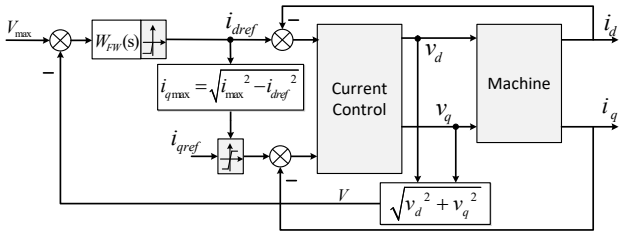

Fig. 12. Direct flux weakening method [4].

There are several flux weakening methods including analytical, advanced angle, and direct current method. Analytical method uses relevant equations to calculate the required reactive power to implement the flux weakening control. However, the performance of this method can be easily affected by the system parameters, such as cable resistance. The advanced angle method means the current reference vector is shifted by an angle to get the demagnetizing current. The advantage is that it requires less information of the machine parameters. But there is no current vector under no load.

The direct current method indicates the demagnetizing current i_{dref} can be controlled directly from a PI controller, namely $W_{FW}(s)$. The control structure is illustrated in Fig.12. The machine terminal voltage is limited to its maximum voltage V_{max} by flux weakening controller $W_{FW}(s)$ which is used to get the reference demagnetizing current i_{dref}. If the machine voltage is below V_{max}, the output of $W_{FW}(s)$ remains to be 0. When the machine voltage is over V_{max}, the output reference current i_{dref} is a negative value with a limit of $-I_{max}$.

There is little literature about the design of flux weakening controller $W_{FW}(s)$. Theoretical analysis points out that proportion gain plays an important role in adjusting the flux weakening controller. The proportion gain should be carefully designed on the basis of system stability. The combination of small signal analysis and root locus is an effective way.

C. Sensorless control technology

The so-called More Electric Engine (MEE) that integrate the S/G directly within the aircraft engine can eliminate gearbox, thus improving reliability and energy conversion efficiency. However, the conventional position sensor is hard to be used because of the harsh environmental and structural constraint. Therefore, it is desirable to develop a sensorless control method. In [18], a sensorless control strategy for embedded PM generator was proposed. The measured stator current is transformed to a single current vector. By combining the magnitude and phase of the current vector with desired voltage magnitude and phase, the voltage vector can be determined. But this method depends on the load condition.

Existing engines employ externally mounted PM machine which are coupled via gearing arrangements. Commonly, the rotor position is sensed using Hall-effect sensors, encodes and resolvers. Hall-effect sensors provide a simple and robust solution, but it does not have high precision at low or zero speed. Encodes present the same disadvantages. Resolves provide accurate rotor position at full speed range but involve the reliability problem at high speed due to the wound rotor component. In order to overcome these problems, sensorless control technology should be adopted [19]. Eliminating the rotor position sensor, the relevant interface circuit and cable can reduce the weight of the whole system and also increase the reliability.

Sensorless control strategies have been widely investigated in the motor drive system, but there is little literature about generation system. In [20] [21], a floating reference frame method which is suitable for both starting and generating mode is proposed. The estimated angle of the floating reference frame can be calculated through the comparison of current vector. The difference between [19] and [20] is the approach of alignment of complex plane and stationary reference frame. Combining this strategy with HRPMM, the reliability of the system can be improved. However, due to the dependence on the current vector, it is difficult to estimate the angle without load.

D. Fault-tolerant machine and converter

1) Suppression of the short circuit current

Short circuit fault of PMS/G includes external fault and internal fault, particularly turn-to-turn fault. The external SC current is usually suppressed by the three-phase symmetrical short circuit at the end of the winding and the high reactance characteristic of the machine.

The HRPMM was conceived to inherently limit the short circuit current to the rated value or slightly higher within the thermal limits of the system. This feature makes the PMS/G system much safer and changes the characteristics of PM machines [17]. However, there is little literature about how to design an HRPMM, which is worth more attention and further studying.

Based on the theory of equivalent circuit of the HRPMM, the phase current Ip is calculated with the expression as follows:

$$I_p = \frac{E}{Z_s + Z_L} = \frac{E}{(\mathrm{R}_s + \mathrm{jX}_s) + [\mathrm{R}_L + \mathrm{j}(\mathrm{X}_L - \mathrm{X}_C)]} \tag{1}$$

In equation (1), E is the back electromotive force of the phase, Z_s and Z_L represent the synchronous impedance of the machine and load impedance respectively. R_s is the winding resistance and X_s is the reactance. The load is represented by resistance R_L, reactance X_L and admittance X_c.

When an external short circuit of the winding occurs, the amplitude of the short circuit current can be obtained from equation (1) by turning the load parameters to zero and the result is shown in equation (2).

$$I_{sc} = \frac{E}{Z_s} = \frac{E}{(\mathrm{R}_s + \mathrm{jX}_s)} \tag{2}$$

From equation (2), it is obvious that the short circuit current is mainly related to E and Z_s which needs to be carefully designed to make sure the short circuit current in an acceptable level. Z_s is composed of R_s and X_s. In most case, R_s is much smaller than X_s at rated speed. So R_s can be ignored for the sake of simplification. Therefore equation (2) is simplified as follows:

$$I_{sc} = \frac{E}{Z_s} = \frac{E}{\mathrm{j}X_s} \tag{3}$$

Fig.13 shows the relationship between machine terminal voltage and machine phase current under different loads when PMS/G works in generating mode.

Curve 1 is the loading characteristic of a conventional PM machines under resistive load only. It is obvious that the voltage drop is small due to the low machine reactance while the short circuit current is much higher. Curve 2 is the HRPMM with resistive load that features the voltage drop is much faster and the short circuit current is much smaller compared to curve 1. Thus, it makes a safe operation when external short circuit fault occurs. However, the ability of power extracting is difficult from this type of machine with resistive load only. Curve 3 is the HRPMM with resistive and capacitive load. It is apparent that more power can be extracted from machine and curve 3 can be adjusted with the voltage dropping as low as curve 1. In practical design, since one value capacitor bank can only satisfy one load point, therefore the role of capacitor is replaced by three phase converter with leading power factor control that provides both steady state and transient response.

High reactance design of PMS/G can limit the short circuit current to the rated value. However, due to high required starting torque, high reactance will increase the inverter VA-rating and required DC bus voltage when starting. The reason is that good starting performance requires high torque-per-ampere rating which in turn requires high flux density in the machine. Thus the short circuit current will not be limited. Therefore, a trade-off should be made between the starting performance and the ability of limiting the fault current.

It should be noted that the suppression of the SC current is carried out under a certain temperature constraint. Thus, the cooling methods, high temperature electrical insulation material, high temperature permanent magnets and demagnetization problem need to be considered as well.

The turn-to-turn SC fault is a severe fault which cannot be easily eradicated. The equivalent circuit is illustrated in Fig.14.

The field of PM machine is established by permanent magnets, which cannot be controlled. Since the resistance and inductance of the single shorted turn are quite small, when turn-to-turn SC fault occurs, the EMF of the shorted turn doesn't change too much. This induces large SC current. The SC current may consequently lead to secondary faults unless the fault is appropriately controlled.

Several methods to handle the turn-to-turn short-circuit faults have been reported in the literature. Some methods involve changing the structure of the PM machines. In [22], it points out that the SC current can be limited by replacing conventional round conductor winding with vertically placed strip winding. The SC current can be limited to normal value regardless of the short turn's position in the slot. However, this method introduces high AC losses during the high speed which is not adoptable in the aircraft starter generator application [23, 24]. It has been shown that rearranging the winding position in

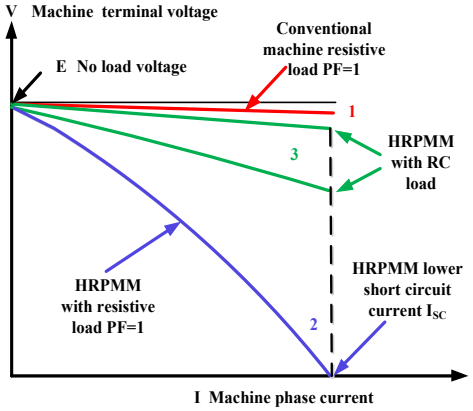

Fig. 13. V/I characteristic of PMSM [16].

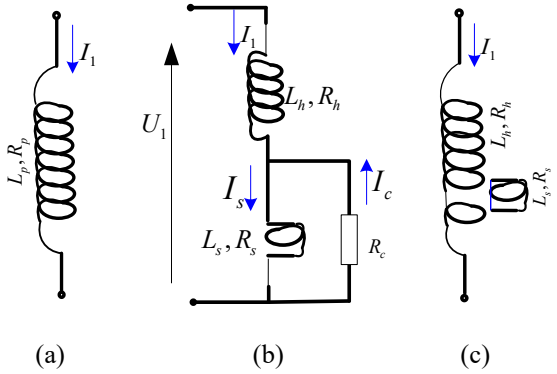

Fig. 14. (a) Healthy coil (b) incipient stage (c) full short circuit stage.

a way to share the slot-leakage flux can also limit the SC current [25]. But the wire wrapping is complex, requiring precise manufacturing. Mechanical shunts [26-28], field windings and electrical shunts [29, 30] are proposed in the literature. They all require additional mechanical or electrical devices, thus lowering the power density of the PMS/G.

Other protection methods focus on the control strategies. In those early days, the most common method is to transform the turn-to-turn SC fault to external SC fault by shorting the terminal of the winding [31, 32]. H-bride inverter topology has been adopted to isolate each phase electrically in case of SC fault. The method can be easily implemented via electronic devices while increasing the number of switches decreasing system reliability. In order to overcome the disadvantages, dual three phase fractional-slot concentrated winding (FSCW) is taken into account [33, 34]. Each winding is connected to an independent inverter. In the event of an SC fault, the faulty winding is shortened and the machine operates by means of the healthy winding only [34]. It maintains comparable performance under fault but the winding should meet certain requirements. For the sake of limiting SC current to the rated value, the inductance of each phase should be designed to 1p.u. leading to the decay of overload capability. Phase current injection technology has been taken as a remedial action [35, 36]. In [35], a bar wound PM motor is discussed. It focuses on the steady-state response and depends on rapid detection of the fault. The airgap flux is nulled to zero in the method proposed

in [36]. The SC current can be controlled effectively but the motor cannot provide any power after the fault.

2) Multi-phase machine design

Fault-tolerant requirements imposed by aircraft application can be met by adopting multiphase single-layer FSCW configuration. Each winding is electrically, magnetically, thermally and mechanically isolated. When a short circuit fault or open circuit fault of the winding occurs, the machine performance will not drop or drop a small part through the corresponding method to isolate the faulted winding. The rest of the healthy windings continue to work. Considering the cost and complexity, the number of the phase is usually no more than six [37]. Generally, five-phase and six-phase PM machines received a lot of attention for the advantages of high controllability, reliability, and smooth torque production in case of a failure [38].

In [39], a six-phase single-layer FSCW PM generator that is directly connected with the low pressure compressor shaft of the aircraft engine is designed. Two sets of three-phase windings are arranged and the corresponding windings are shifted of 60 electrical degrees. The permanent magnet material Sm2Co17 is utilized to withstand the high temperature environment inside the aircraft engine. The main design parameters are shown in Table III.

In [40], a 250kW five-phase permanent magnet generator for the low-pressure shaft of a large civil engine is designed. The chosen of five-phase involves a degree of judgment in terms of factors such as reliability, cost and complexity. A machine with 28 rotor poles and 40 stator slots was chosen on the basis of the requirements for low mutual coupling, low rotor electromagnetic losses and low machine mass. The main design parameters are shown in Table IV.

The multiphase machines are capable of continuing to operate at or near rated power in case of a failure within the machine or its converter. The phase windings are therefore isolated magnetically, thermally and physically [40]. Thus, the converter must be also independent to minimize the potential for fault propagation. The H-bridge converter that combines each phase and four power switches is chosen.

The H-bridge converter functions in three patterns. The first one is pure diode rectification. During the pattern, the power switches Q1-Q4 don't work while the diodes D1-D4 work. The second pattern is called power factor correction (PFC). During the pattern, the phase current is sinusoidal shaped. The phase current and the phase voltage are in phase, so the power factor is 1. The converter functions in the boost way. It can be classified into four modes, as can be seen in Fig.15. The third pattern is called phase shifting. It utilizes the armature reaction to keep the output voltage constant regardless of the speed and the load [41].

3) Fault-tolerant topologies of the converter

The power switch may also fails during the operation. The fault types include open circuit fault and short circuit fault.

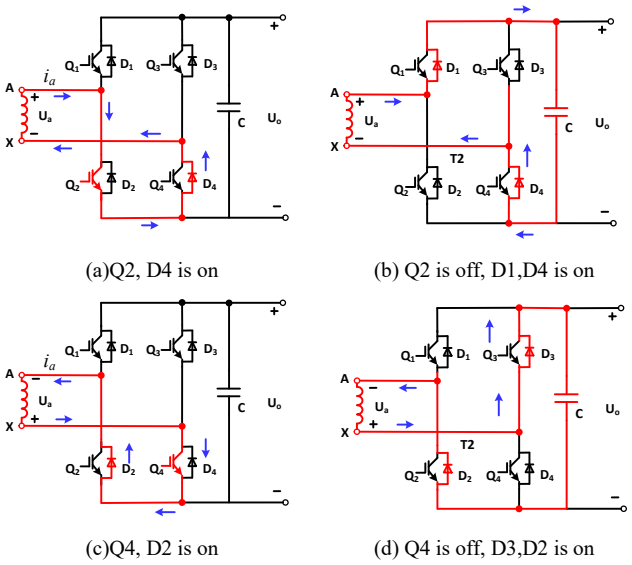

Fig. 15. Four modes in PFC pattern [41].

TABLE III
MAIN DESIGN PARAMETERS IN SIX-PHASE CONFIGURATION

Parameter	Requirement
Rated torque	40N.m
Rated speed	2400rpm
Rated voltage	60V
Rated current	31Arms
Number of poles	28
Number of slots	24
Internal diameter	178mm
External diameter	300mm
Active axial length	44mm
Airgap length	2mm

TABLE IV
MAIN DESIGN PARAMETERS IN FIVE-PHASE CONFIGURATION

Parameter	Requirement
Rated power	250kW
Speed range	1050-3100rpm
Cooling	Bypass air
Coil per phase	4
Stator outer diameter	554mm
Stator slot depth	53mm
Stator and rotor axial length	185mm
Airgap length	3mm
Magnets	Sm_2Co_{17}
Number of series turns per coil	8

Generally, the method to solve these problems is to adopt the fault-tolerant converter. That means once a fault occurs, the

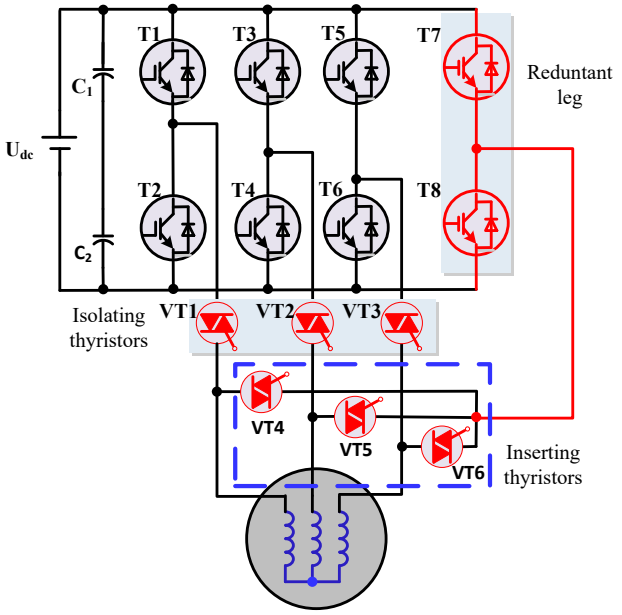

Fig. 16. Winding connect to the extra bridge.

power switch must be isolated and the converter is reconfigured. The relevant control strategy can guarantee that the machine still deliver certain power.

In [42], a fault-tolerant converter with a redundant leg is presented. The topology is shown in Fig.16. The redundant leg is not used when the machine works at normal condition. The isolating thyristors that comprised of three back-to-back connected thyristors are used to isolate the faulted leg and the inserting thyristors are used to inserting the redundant leg. Although this fault-tolerant topology is analyzed for motor drive system, it is also applicable for generation system to maintain a certain power output in the event of the power switch failure in EPS for aircraft.

Other topologies and their features are shown in Table V. However, all these topologies are investigated for motor drive system rather than generation system. Notably, the H-bridge converter is a common fault tolerant topology for multiphase machine in generating mode .The application of the topologies mentioned in Table V for aircraft EPS needs to be further analyzed and discussed.

It is worth noting that electrolytic power capacitors are the key components which determine the life cycle of the whole system and substantially are responsible for converter breakdown failures [52]. The electrolytic capacitors hold the maximum distribution of possible failures compared to other components, such as IGBTs and power diodes [53]. To avoid the failure of the electrolytic capacitor, online monitoring method has been proposed, which detects the end-of-life status of the capacitor to allow a timely replacement [52]. For example, in [54], estimation of the equivalent series resistance (ESR) of the capacitor with recursive least square (RLS) method is proposed. The increase of the ESR is very pronounced as compared to the capacitance value. This method can provide a quick and accurate estimation with minimum hardware requirements.

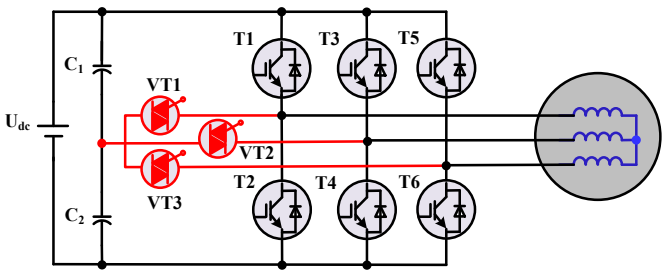

Fig. 17. Winding connected to the neutral point of capacitor.

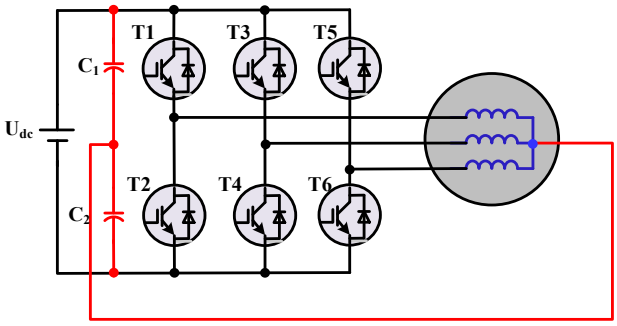

Fig. 18. Winding neutral point connected to the neutral point of capacitor.

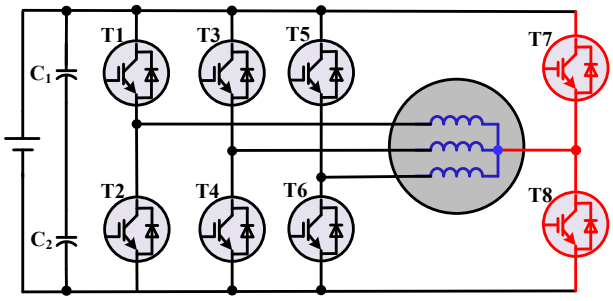

Fig. 19. Winding neutral point connected to the extra bridge.

TABLE V
FAULT TOLERANT TOPOLOGIES OF THE CONVERTER

Fault-tolerant topologies	Features	Ref.
Winding connected to the neutral point of the capacitor	Fig.17. Simple structure; no additional hardware; maximum speed reduced to the half of the rated speed	43-45
Winding neutral point connected to the neutral point of the capacitor	Fig.18. maximum torque reduced to the $1/\sqrt{3}$ of the rated torque	46-48
Winding neutral point connected to the extra bridge	Fig.19. speed remains; maximum torque reduced to the $1/\sqrt{3}$ of the rated torque	49-51

4) Fault protection technology

There is a need for method to prevent damage to PM machines and to any downstream components in the event of a failure. A method called machine neutral decoupling is

proposed in [55]. Each winding is connected to the neutral point through a fault protector comprised of three bi-directional switches. The winding current detected by the current sensors increases a lot when a short circuit fault occurs. Then bi-directional switch opens to force winding current to zero. This method not only ensures the safe operation of the machine, but also ensures the safety of the converter and the loads. Another method called thermal protection is found in [56]. Ferrite material is used in the stator and rotor. This material heats up due to the high fault current and becomes non-magnet in case of a fault. When cooled down, the material regains the magnetic properties. However, the magnetic properties of this material is poor which reduces the power density of the machine and the speed of the stator and rotor becoming non-magnetic also affects the limitation of the fault current. In [57], a magnetic fluid is adopted as part of the magnetic circuit and also as the coolant to the system. The fluid can be pumped out to interrupt the magnetic circuit and then the fault current can be limited. The weakness of this method is the low permeability of the magnetic fluid which reduces the power density of the machine.

E. Wide BandGap Semiconductor Based Converter

The MEA concept involves the increasing demand of electrical power that forces the development of converter with high efficiency and high power density. As for S/G system, the converter with high efficiency and high power density can limit temperature rising in the starting mode and can increase efficiency in the generating mode.

Generally, higher efficiency can be achieved by reducing the converter total losses, and higher power density can be achieved by increasing the switching frequency of the converter so as to reduce the size of passive components [58].These two requirements can be implemented by using Wide BandGap (WBG) semiconductors. In fact, Silicon Carbide (SiC) semiconductors are the promising candidate to replace the Silicon semiconductor [59]. The efficiency of SiC converters are much better than Si converters due to the inherently lower conduction and switching losses [60]. Moreover, SiC semiconductors can operate at higher junction temperature compared to Si semiconductors, which reduce the volume and weight of the cooling system.

In [58], the performance of the 1200V/100A SiC MOSFET power module is evaluated in a three phase 540V-45kVA inverter used for MEA. An equivalent Si IGBT power module is also considered in the comparison for two different switching frequencies, 15 kHz and 60 kHz. The switching and conduction losses of the Si IGBT power module are almost eight times of the SiC MOSFET power module at high switching frequency. But at low switching frequency the advantage of using SiC is not so obvious.

In [61], a performance assessment of different converter topologies for PMS/G is presented. The simulation is carried out in generating mode that considers both 2-Levels and 3-Levels converter structure. The power module is based on Si and SiC technology. The simulation results have shown that the efficiency of SiC-based module is much higher than conventional IGBT power module at the same switching frequency.

V. FLUX-WEAKENING PROTECTION DEALING WITH TURN-TO-TURN SHORT CIRCUIT FAULT

A. Control principle

In order to limit the turn-to-turn SC current, a flux-weakening protection strategy is proposed. It is implemented by injecting the negative d-axis current. The control strategy can be separated into two modes: the starting mode and the generating mode. Both the two modes not only meet the basic requirements but can also limit turn-to-turn SC current to a permissible level. Fig.20 and Fig.21 depict the control structure. Both structures use the same bi-directional three-phase bridge converter for reducing the weight and increasing the power density of the PMS/G system.

The direct control of airgap flux is not available, however, the armature reaction can be utilized. Injecting current aligned with negative d-axis (i_d) generates flux linkage opposite to that of the PMs in the airgap. Consequently, the EMF of the shorted turns is reduced, taking SC current under control. This technique is called flux-weakening protection. Based on the theory, when the machine operates in the normal condition, the given value of i_d is zero. When SC fault takes place, the given value of i_d is negative.

The control structure in starting mode contains two loops. The outer loop is speed regulation loop. Comparing the command speed to the measured speed, the PI controller transforms the differences to the command value of q-current. The inner loop is current regulation loop, making the measured current track on the command. The turn-to-turn SC fault detection module detects the harmonics of the phase currents to tell if the SC fault happens. When the fault doesn't take place, the number of short circuit turns is zero. The command value of i_d is zero. When the turn-to-turn SC fault occurs, the detection module calculates the number of short circuit turns and sends the information to the command current calculation module. The command i_d is decided according to the speed, the iq current and the number of short circuit turns. The value is negative to limit the turn-to-turn SC current. The current controller outputs the command value of d-axis voltage and q-axis voltage. The SVPWM is employed to calculate the PWM signals to drive the IGBTs.

In the generating mode, three phase controlled rectifier is employed. The output voltage is regulated to 270V DC to satisfy the configuration of HVDC electrical power system in the aircraft. The objective in this mode is to control the dc-link voltage within a certain range. The machine speed is no longer a control variable but an external variable determined by the aircraft engine. The outer loop regulates output voltage instead of speed, affecting the command value of q-current. The inner loop is similar to the starting mode.

B. Finite element simulation and experiment verification

To validate the proposed method, finite element simulation and experiments are conducted on a 24-slot, 16-pole PMSM with 70A rated phase current. Fig.22 shows the cross sectional view of the PM machine. A fractional slot concentrated winding configuration with spoke-type rotor structure is adopted due to the advantage of relatively small short circuit current [62].

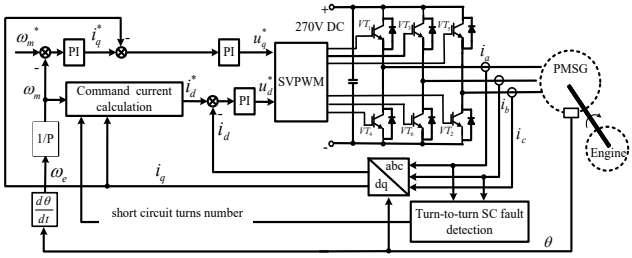

Fig. 20. Flux-weakening protection principle in motoring mode.

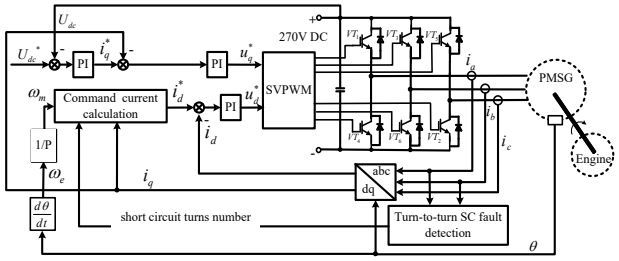

Fig. 21. Flux-weakening protection principle in generating mode.

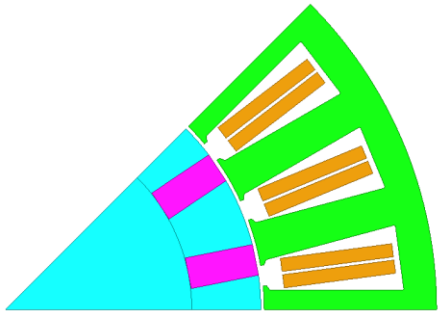

Fig. 22. Quarter cross sectional view of a 24-slot, 16-pole PMSM.

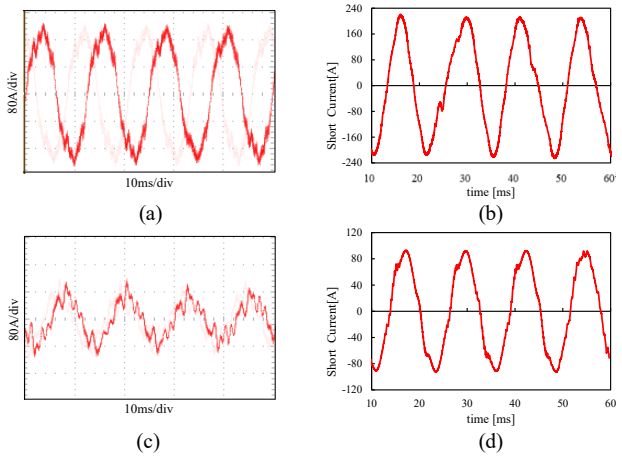

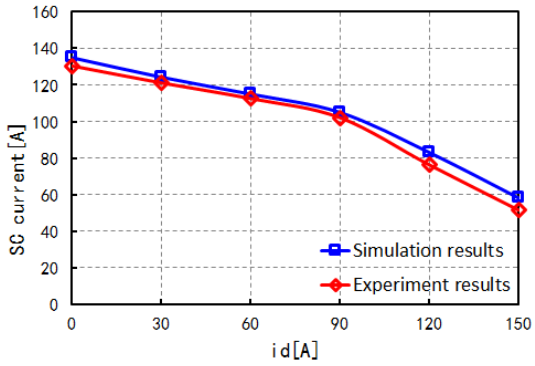

Fig. 23. The simulation and experiment SC current with the flux weakening protection.(a) the experiment SC current under i_d =0A (b)the simulation SC current under i_d=0A (c) the experiment SC current under i_d =150A (d) the experiment SC current under i_d =150A (e)the simulation and experiment SC currents under different i_d.

For the consideration of coils safety, the machine functions at 600rpm for verification. Different i_d is injected to observe the SC current. Fig.23 illustrates the SC currents in simulation and experiment. The experiment results are in accordance with the simulation results. When the i_d current increases from 0A to 150A, the SC current can be decreased from 130.5A to 51.4A. The experiment results indicate that the SC current can be controlled under the rated value when the proper current i_d is applied.

VI. CONCLUSION

This paper presents an overview of the state-of-the-art and development of PMS/G for aircraft EPS application. The key technologies to implement the PMS/G system are also analyzed. The flux weakening protection strategy dealing with the turn-to-turn SC fault is presented in detail.

The main barrier of PM machines in aircraft application is the de-excitation problem in the event of a failure. HRPMM compensates for this defect due to the inherent limitation of the SC current. Meanwhile, the cooling methods, high temperature electrical insulation materials, high temperature permanent magnets and demagnetization problem should be systematically considered for implementation of the HRPMM. Another approach is to develop the innovative hybrid excitation machines, which combine the advantages of PM machines with the controllability of the magnetic flux by auxiliary field windings.

The multiphase PM machines together with H-bridge converters increase the fault-tolerant ability whether the machine is externally mounted or embedded in the aircraft engine.

With the breakthrough of the key technologies based on the development of advanced electromagnetic material, high temperature semiconductor and cooling system, especially the oil cooling method, high power density PM machines will be a competitive candidate for the starter-generator, even embedded starter/generator application in EPS of aircraft.

REFERENCES

[1] Weimer, "Past, Present & Future Aircraft Electrical Power Systems", *in Proc. 39th Aerospace Sciences meeting*, Nevada, January, 2001.

[2] Ian Moir and Allan Seabridge, Aircraft Systems: Mechanical, electrical, and avionics subsystems integration, 3rd ed. Chichester, U.K.: John Wiley & Sons Ltd, 2008, ch5, pp.181-184.

[3] G. Friedrich and A. Girardin, "Integrated starter generator," *IEEE Ind. Appl. Mag.*, vol. 15, no. 4, pp. 26–34, Jul.–Aug. 2009.

[4] L. Alberti et al., "IPM machine drive design and tests for an integrated starter–alternator application," *IEEE Trans. Ind. Appl*., vol. 46, no. 3,pp. 993–1001, May-Jun. 2010.

[5] Bozhko, S. S. Yeoh, F. Gao and C. Hill. "Aircraft starter-generator system based on permanent-magnet machine fed by active front-end rectifier," *in Proc. IEEE IECON 2014 - 40th Annual Conference of the IEEE Industrial Electronics Society,* Dallas, TX, 2014, pp. 2958-2964.

[6] S. S. Yeoh, F. Gao, S. Bozhko and G. Asher. "Control design for PMM-based starter generator system for More Electric Aircraft," *in Proc. 16th European Conference on Power Electronics and Applications*, 2014, pp. 1-10.

[7] F. Gao, S. Bozhko, Y. Seang Shen and G. Asher. "Control design for PMM starter-generator operated in flux-weakening mode," *in Proc. 2014 16th European Conference on Power Electronics and Applications, Lappeenranta,* 2014, pp. 1-10.

[8] Puvan Arumugam, Chris Gerada, Serhiy Bozhko, He Zhang. "Permanent Magnet Starter-Generator for Aircraft Application," *SAE Tech. Pap*.2014-01-2157, 2014.

[9] P. Arumugam et al., "Comparative design analysis of Permanent Magnet rotor topologies for an aircraft starter-generator," *in Proc. IEEE IEPS*, Kyiv, 2014, pp. 273-278.

[10] M. van der Geest, H. Polinder, J. A. Ferreira and D. Zeilstra. "Machine selection and initial design of an aerospace starter/generator," *in Proc. 2013 International Electric Machines & Drives Conference,* Chicago, IL, 2013, pp. 196-203.

[11] D. Papaoikonomou, M. van der Geest and H. Polinder. "Comparison between induction and PM machine for high speed starter-generator applications," *in Proc. 7th IET International Conference on Power Electronics, Machines and Drives (PEMD 2014),* Manchester, 2014, pp. 1-6.

[12] M. van der Geest, H. Polinder, J. A. Ferreira and D. Zeilstra. "Design and testing of a high-speed aerospace permanent magnet starter/generator," *in Proc. 2015 International Conference on Electrical Systems for Aircraft, Railway, Ship Propulsion and Road Vehicles (ESARS),* Aachen, 2015, pp. 1-6.

[13] M. Degano et al. "An optimized bi-directional, wide speed range electric starter-generator for aerospace application," *in Proc. 7th IET International Conference on Power Electronics, Machines and Drives (PEMD 2014),* Manchester, 2014, pp. 1-6.

[14] Ganev, E. and Koerner, M. "Power and Thermal Management for Future Aircraft," *SAE Tech. Pap*. 2013-01-2273, 2013.

[15] Genève. "Advanced Electric Generators for Aerospace More Electric Architectures," *SAE Tech. Pap*. 2010-01-1758, 2010.

[16] Koerner, M, Ganev, E, and Freudenberger, J. "A Turbine-Driven Electric Power Generation System for Launch Vehicles & Other High-Power Aerospace Applications," *SAE Tech. Pap*. 2004-01-3185, 2004.

[17] Ganev, E, "High-Reactance Permanent Magnet Machine for High-Performance Power Generation Systems," *SAE Tech. Pap*. 2006-01-3076, 2006.

[18] S. G. Burrow, P. H. Mellor, P. Churn, T. Sawata and M. Holme. "Sensorless Operation of a Permanent-Magnet Generator for Aircraft," *IEEE Trans. Ind. Appl*., vol. 44, no. 1, pp. 101-107, January.-February. 2008.

[19] A. S. Budden, R. Wrobel, D. Holliday, P. H. Mellor and P. Sangha, "Sensorless Control of Permanent Magnet Machine Drives for Aerospace Applications," *in Proc. International Conference on Power Electronics and Drives Systems*, 2005, pp. 372-377.

[20] Huggett C. E, Kalman G. Floating Frame Controller: U.S. Patent No. 6, 301,136, October, 2001.

[21] Sarlioglu B, Huggett C. E. Decoupling of Cross Coupling for Floating Reference Frame Controllers for Sensorless Control of Synchronous Machines: U.S. Patent No.6, 940, 251, September, 2005.

[22] P. Arumugam, T. Hamiti, C. Brunson and C. Gerada, "Analysis of Vertical Strip Wound Fault-Tolerant Permanent Magnet Synchronous Machines," *IEEE Trans. Ind. Electron.*, vol. 61, no. 3, pp. 1158-1168, March 2014.

[23] P. Arumugam, T. Hamiti and C. Gerada, "Analytical modeling of a vertically distributed winding configuration for Fault Tolerant Permanent Magnet Machines to suppress inter-turn short circuit current limiting," *in Proc. IEEE IEMDC*, Niagara Falls, 2011, pp. 371-376.

[24] P. Arumugam, T. Hamiti and C. Gerada, "Fault tolerant winding design — A compromise between losses and fault tolerant capability," *in Proc. International Conference on Electrical Machines*, Marseille, 2012, pp. 2559-2565.

[25] P. Arumugam, "Design Optimization on Conductor Placement in the Slot of Permanent Magnet Machines to Restrict Turn–Turn Short-Circuit Fault Current," *IEEE. Trans. Mag*., vol. 52, no. 5, pp. 1-8, May 2016.

[26] Glennon. e. al, Permanent magnet generator with fault detection: US Patent 4641080, Feb 3, 1987.

[27] K. D. e. al, Method and apparatus for controlling an electric machine: US Patent 7443070, Oct 28, 2008.

[28] Manoj Ramprasad Shah e. al, Fault-tolerant permanent magnet machine with reconfigurable flux paths in stator back iron: US Patent 7541705, Jun 2, 2009.

[29] A. F. e. al, Flux shunt wave shape control arrangement for permanent magnet machines: US Patent 6750628, Jun 15, 2004.

[30] J. F. G. e. al, Permanent magnet electric generator with variable magnet flux excitation: US Patent 7859231, Dec 28, 2010.

[31] J. A. Haylock, B. C. Mecrow, A. G. Jack and D. J. Atkinson, "Operation of fault tolerant machines with winding failures," *IEEE Trans. Energy Convers.*, vol. 14, no. 4, pp. 1490-1495, Dec 1999.

[32] B. C. Mecrow, A. G. Jack, J. A. Haylock and J. Coles, "Fault-tolerant permanent magnet machine drives," *in Proc. Electric Power Applications*, vol. 143, no. 6, pp. 437-442, Nov 1996.

[33] M. O. E. Aboelhassan, T. Raminosoa, A. Goodman, L. De Lillo and C. Gerada, "Performance Evaluation of a Vector-Control Fault-Tolerant Flux-Switching Motor Drive," *IEEE Trans. Ind. Electron*., vol. 60, no. 8, pp. 2997-3006, Aug. 2013.

[34] M. Barcaro, N. Bianchi and F. Magnussen, "Faulty Operations of a PM Fractional-Slot Machine With a Dual Three-Phase Winding," *IEEE Trans. Ind. Electron*., vol. 58, no. 9, pp. 3825-3832, Sept. 2011.

[35] A. J. Mitcham, G. Antonopoulos and J. J. A. Cullen, "Implications of shorted turn faults in bar wound PM machines," *in Proc. Electric Power Applications*, vol. 151, no. 6, pp. 651-657, 7 Nov. 2004.

[36] B. A. Welchko, J. Wai, T. M. Jahns and T. A. Lipo, "Magnet-flux-ing control of interior PM Machine drives for improved steady-state response to short-circuit faults," *IEEE Trans. Ind. Appl*., vol. 42, no. 1, pp. 113-120, Jan.-Feb. 2006.

[37] W. Cao, B. C. Mecrow, G. J. Atkinson, J. W. Bennett and D. J. Atkinson, "Overview of Electric Motor Technologies Used for More Electric Aircraft (MEA)," *IEEE Trans. Ind. Electron*., vol. 59, no. 9, pp. 3523-3531, Sept. 2012.

[38] A. M. EL-Refaie, M. R. Shah and K. K. Huh, "High-Power-Density Fault-Tolerant PM Generator for Safety-Critical Applications," *IEEE Trans. Ind. Appl.*, vol. 50, no. 3, pp. 1717-1728, May-June 2014.

[39] A. Cavagnino, Z. Li, A. Tenconi and S. Vaschetto, "Integrated Generator for More Electric Engine: Design and Testing of a Scaled-Size Prototype," *IEEE Trans. Ind. Appl.*, vol. 49, no. 5, pp. 2034-2043, Sept.-Oct. 2013.

[40] Jason Ede, Geraint Jewell, Kais Atallah, David Powell, John Cullen, and Alan Mitcham. "Design of a 250kW, Fault-Tolerant PM Generator for the More-Electric Aircraft", *in Proc.3th International Energy Conversion Engineering Conference*, California, 2005.

[41] Haihong Qin, Yangguang Yan, Power system for More Electric Aircraft. Beijing: Beihang University Press, 2016, pp.282-284.

[42] R. R. Errabelli and P. Mutschler, "Fault-Tolerant Voltage Source Inverter for Permanent Magnet Drives," *IEEE Trans. Power Electron.*, vol. 27, no. 2, pp. 500-508, Feb. 2012.

[43] J. O. Estima and A. J. M. Cardoso. "A fault-tolerant permanent magnet synchronous motor drive with integrated voltage source inverter open-circuit faults diagnosis," *in Proc.14th European Conference on Power Electronics and Applications*, Birmingham, 2011, pp. 1-10.

[44] J. Klima. "Analytical Investigation of an Induction Motor Fed From Four-Switch VSI With a New Space Vector Modulation Strategy," *IEEE Trans. Energy Convers*., vol. 21, no. 4, pp. 832-838, Dec. 2006.

[45] J. O. Estima and A. J. M. Cardoso. "Efficiency evaluation of fault-tolerant operating strategies applied to three-phase permanent magnet synchronous motor drives," *in Proc. International Conference on Electrical Machines*, Marseille, 2012, pp. 2411-2417.

[46] M. Beltrao de Rossiter Correa, C. Brandao Jacobina, E. R. Cabral da Silva and A. M. Nogueira Lima. "An induction motor drive system with improved fault tolerance," *IEEE Trans. Ind. Appl*., vol. 37, no. 3, pp. 873-879, May/Jun 2001.

[47] K. D. Hoang, Z. Q. Zhu, M. P. Foster and D. A. Stone. "Comparative study of current vector control performance of alternate fault tolerant inverter topologies for three-phase PM brushless ac machine with one phase open circuit fault," *in Proc. 5th IET International Conference on Power Electronics*, *Machines and Drives*, Brighton, UK, 2010, pp. 1-6.

[48] D. U. Campos-Delgado, D. R. Espinoza-Trejo and E. Palacios. "Fault-tolerant control in variable speed drives: a survey," *IET Elect. Power App*., vol. 2, no. 2, pp. 121-134, March 2008.

[49] O. Wallmark, L. Harnefors and O. Carlson. "Post-fault operation of fault-tolerant inverters for PMSM drives," *in Proc. European Conference on Power Electronics and Applications*, Dresden, 2005, pp. 10-11.

[50] O. Wallmark, L. Harnefors and O. "Carlson. Control Algorithms for a Fault-Tolerant PMSM Drive," *IEEE Trans. Ind. Electron*., vol. 54, no. 4, pp. 1973-1980, Aug. 2007.

[51] S. Bolognani, M. Zordan and M. Zigliotto. "Experimental fault-tolerant control of a PMSM drive," *IEEE Trans. Ind. Electron*., vol. 47, no. 5, pp. 1134-1141, Oct 2000.

[52] M. A. Vogelsberger, T. Wiesinger and H. Ertl, "Life-Cycle Monitoring and Voltage-Managing Unit for DC-Link Electrolytic Capacitors in PWM Converters," *IEEE Trans. Power Electron*., vol. 26, no. 2, pp. 493-503, Feb. 2011.

[53] Hao Ma and Linguo Wang, "Fault diagnosis and failure prediction of aluminum electrolytic capacitors in power electronic converters," *in Proc. IEEE IECON,* Raleigh, NC, 2005, pp.842-847.

[54] Y. Yu, T. Zhou, M. Zhu and D. Xu, "Fault Diagnosis and Life Prediction of DC-link Aluminum Electrolytic Capacitors Used in Three-phase AC/DC/AC Converters," *in Proc. Second International Conference on Instrumentation, Measurement, Computer, Communication and Control*, Harbin, 2012, pp. 825-830.

[55] Ganev E. D, Bansal M. L, and Warr W. H. System and Method for Fault Protection for Permanent Magnet Machines: U.S. Patent No. 7,276,871.

[56] Keizo H. Liquid-cooled electromagnetic machine: JP2000236649A2, 29, August, 2000.

[57] A. Chen, R. Nilssen and A. Nysveen, "Performance comparisons among radial flux, multi-stage axial flux and three-phase transverse flux PM machines for downhole applications," *in Proc. IEEE International Electric Machines and Drives Conference*, Miami, FL, 2009, pp. 1010-1017.

[58] A. Hilal, B. Cougo and T. Meynard, "Characterization of high power SiC modules for more Electrical Aircrafts," *in Proc. IEEE IECON,* Florence, 2016, pp. 1087-1092.

[59] J. Biela, M. Schweizer, S. Waffler, J. W. Kolar, "SiC versus Si Evaluation of Potentials for Performance Improvement of Inverter and DC-DC Converter Systems by SiC Power Semiconductors," *IEEE Tran. Ind. Electron*., vol. 58, No. 7, pp. 2872-2882, July 2011.

[60] R. Wang, D. Boroyevich, P. Ning, Z. Wang, F. Wang, P. Mattavelli, K.N go, and K. Rajashekara, "A high-temperature SiC three-phase ac-dc converter design for > 100°C ambient temperature, " *IEEE Tran. Power Electron*., vol. 28, no. 1, pp. 555–572, Jan. 2013.

[61] G. L. Calzo, P. Zanchetta, C. Gerada, A. Gaeta and F. Crescimbini, "Converter topologies comparison for more electric aircrafts high speed Starter/Generator application," *in Proc. IEEE ECCE*, Montreal, QC, 2015, pp. 3659-3666.

[62] Lijun Zhou, Yongmei Wu, Weiwei Geng, Zhuoran Zhang, Chuang Liu, "Comparative Study on Concentrated-Windings Permanent Magnet Synchronous Machines with Different Rotor Structures for Aircraft Generator Application," *in Proc. 18th International Conference on Electric Machines and Systems (ICEMS'2015)*, Pattaya, Thailand, Oct, 2015.

Zhuoran Zhang (M'09–SM'12) received the B.S. degree in measurement engineering and the M.S. and Ph.D. degrees in electrical engineering from Nanjing University of Aeronautics and Astronautics (NUAA), Nanjing, China, in 2000, 2003 and 2009, respectively. Since 2003, he has been a member of the faculty at Department of Electrical Engineering, NUAA, where he is currently a professor and vice director of Jiangsu Provincial Key Laboratory of New Energy Generation and Power Conversion. From Feb. 2012 to Jun. 2013, he was a visiting professor in Wisconsin Electric Machines and Power Electronics Consortium (WEMPEC), University of Wisconsin-Madison, U.S.

His research interests include design and control of permanent magnet machines, hybrid excitation electric machines, and doubly salient electric machines for aircraft power, electric vehicles, and renewable energy generation. He has authored or coauthored over 90 technical papers and one book, and is the holder of 25 issued patents in these areas.

Jian Huang received the B.S. degree in measurement engineering and the M.S. degree in automation engineering from Anhui University, Hefei, China, in 2012 and 2015, respectively. He is working towards his PhD. degree in electrical engineering in Nanjing University of Aeronautics and Astronautics.

His research interest focuses on the starter/generator system of permanent magnet machines for aircraft electrical power systems.

Yunyi Jiang received the B.S. degree in electrical engineering from Nanjing University of Aeronautics and Astronautics, Nanjing, China, in 2016. She is working towards her master degree in Nanjing University of Aeronautics and Astronautics.

Her research interest focuses on the permanent magnet starter/generator system for the MEA.

Weiwei Geng received the B.S. degree in electrical engineering from Nanjing Agriculture University, Nanjing China, in 2011 and the M.S. degree in electrical engineering from NUAA, Nanjing, China, in 2014. He is working towards his PhD. degree in electrical engineering in Nanjing University of Aeronautics and

Astronautics.

His main research interests include permanent-magnet motors and generators for aircraft power and electric vehicles and the control of stators/generators for hybrid excitation machines.

Yanwu Xu(S'16) received the B.S. degree in measurement engineering and the M.S. degree in automation engineering from Anhui University, Hefei, China, in 2012 and 2015, respectively. He is working towards his PhD. degree in electrical engineering in Nanjing University of Aeronautics and Astronautics.

His research interest focuses on the electrical power generation and the micro grid for the MEA.